The Relationship between Mating System and Genetic Diversity in Diploid Sexual Populations of *Cyrtomium falcatum* in Japan

Ryosuke Imai[1]☯, Yoshiaki Tsuda[2]☯, Sadamu Matsumoto[3], Atsushi Ebihara[3], Yasuyuki Watano[1]*

1 Department of Biology, Graduate School of Science, Chiba University, Yayoi, Inage, Chiba, Japan, **2** Sugadaira Montane Research Center, University of Tsukuba, Ueda, Nagano, Japan, **3** Department of Botany, National Museum of Nature and Science, Tsukuba, Ibaraki, Japan

☯ These authors contributed equally to this work.
* watano@faculty.chiba-u.jp

Abstract

The impact of variation in mating system on genetic diversity is a well-debated topic in evolutionary biology. The diploid sexual race of *Cyrtomium falcatum* (Japanese holly fern) shows mating system variation, i.e., it displays two different types of sexual expression (gametangia formation) in gametophytes: mixed (M) type and separate (S) type. We examined whether there is variation in the selfing rate among populations of this species, and evaluated the relationship between mating system, genetic diversity and effective population size using microsatellites. In this study, we developed eight new microsatellite markers and evaluated genetic diversity and structure of seven populations (four M-type and three S-type). Past effective population sizes (Ne) were inferred using Approximate Bayesian computation (ABC). The values of fixation index (F_{IS}), allelic richness (A_R) and gene diversity (h) differed significantly between the M-type (F_{IS}: 0.626, A_R: 1.999, h: 0.152) and the S-type (F_{IS}: 0.208, A_R: 2.718, h: 0.367) populations (when admixed individuals were removed from two populations). Although evidence of past bottleneck events was detected in all populations by ABC, the current N_e of the M-type populations was about a third of that of the S-type populations. These results suggest that the M-type populations have experienced more frequent bottlenecks, which could be related to their higher colonization ability via gametophytic selfing. Although high population differentiation among populations was detected ($F_{ST} = 0.581$, $F'_{ST} = 0.739$), there was no clear genetic differentiation between the M- and S-types. Instead, significant isolation by distance was detected among all populations. These results suggest that mating system variation in this species is generated by the selection for single spore colonization during local extinction and recolonization events and there is no genetic structure due to mating system.

Introduction

The diversity of mating and sexual systems in land plants is of great interest to evolutionary biologists. For seed plants, the presence of both male and female reproductive organs within a single individual (i.e. monoecy) is a common and ancestral state [1]. Thus, seed plants are potentially faced with a strategic decision of whether to reproduce through outcrossing, selfing, or mixed mating, which is a mixture of outcrossing and selfing [2]. In the short term, selfing is favored due to transmission advantage [3] and reproductive assurance [4,5]. However the progeny derived from selfing may suffer inbreeding depression [6]. The relative balance between these advantages and disadvantages strongly influences mating system evolution. In this respect, the correlation between the evolution of selfing and severe genetic drift events such as bottlenecks is important because both the transmission advantage [3] and reproductive assurance [4,5] theories predict their co-occurrence. The former theory predicts that population bottleneck events that result in the purging of inbreeding depression would trigger the evolution of selfing [7], while in the latter theory, selfing would be favored under limited mating opportunities, which are expected in colonization processes. Thus, if populations display mating system variation, reduction of effective population size is expected, due to the co-occurrence of selfing and bottlenecks [8]. However, this scenario has not been well examined in either gymnosperm or pteridophyte species. The mating systems of homosporous pteridophytes are of interest because they are unique among vascular plants; their free-living haploid gametophytes can bear both male and female gametangia (antheridia and archegonia) and they are capable of three types of mating systems: gametophytic selfing (i.e. syngamy of gametes derived from the same gametophyte; this extreme form of inbreeding is not possible in heterosporous plants), sporophytic selfing (i.e. syngamy of gametes from two gametophytes that developed from separate spores from the same parent sporophyte; this is analogous to selfing in seed plants), and outcrossing (i.e. syngamy of gametes from two gametophytes derived from separate sporophytes) [9,10]. In order to deepen our understanding of the evolution of mating systems in plants, it is important to examine the correlation between mating system and genetic diversity in homosporous pteridophytes, which are uniquely capable of extreme inbreeding via gametophytic selfing.

In this study, we focused on Japanese holly fern, *Cyrtomium falcatum* (L.f.) C.Presl (Dryopteridaceae), to evaluate the relationship among sexual expression of gametophytes, mating system and genetic diversity. Matsumoto (2003) [11] divided the sexual diploid cytotype of *Cyrtomium falcatum* in Japan into northern and southern types. The northern type is distinguished from the southern type by smaller blades, fewer pairs of pinnae, and grayish indusia without a blackish brown center [11]. The northern type grows on coastal rocks or cliffs and is distributed discontinuously from the southern part of Hokkaido Island to Shikoku Island [11], while the southern type is distributed across the Okinawa Islands, Kyusyu Island and Ogasawara Islands (Fig 1). Matsumoto (2003) [11] observed variation in the sexual expression of the northern type of *C. falcatum*. Sporophytes called mixed type (M-type) simultaneously produce gametophytes with both antheridia (male gametangia) and archegonia (female gametangia) at frequencies of 90% or greater after three months in cultivation. In contrast, sporophytes of the separate type (S-type) produce these bisexual gametophytes at frequencies of 10% or less. This sexual expression is equivalent to dichogamy, in which an individual temporally staggers the development of gametangia, because the gametophytes produce antheridia in the early stages of development and then produce archegonia after releasing sperm. Sporophytes that produce intermediate frequencies (10% < frequency < 90%) of gametophytes that produce antheridia and archegonia simultaneously are considered to be the intermediate type (I-type). Matsumoto (2003) [11]
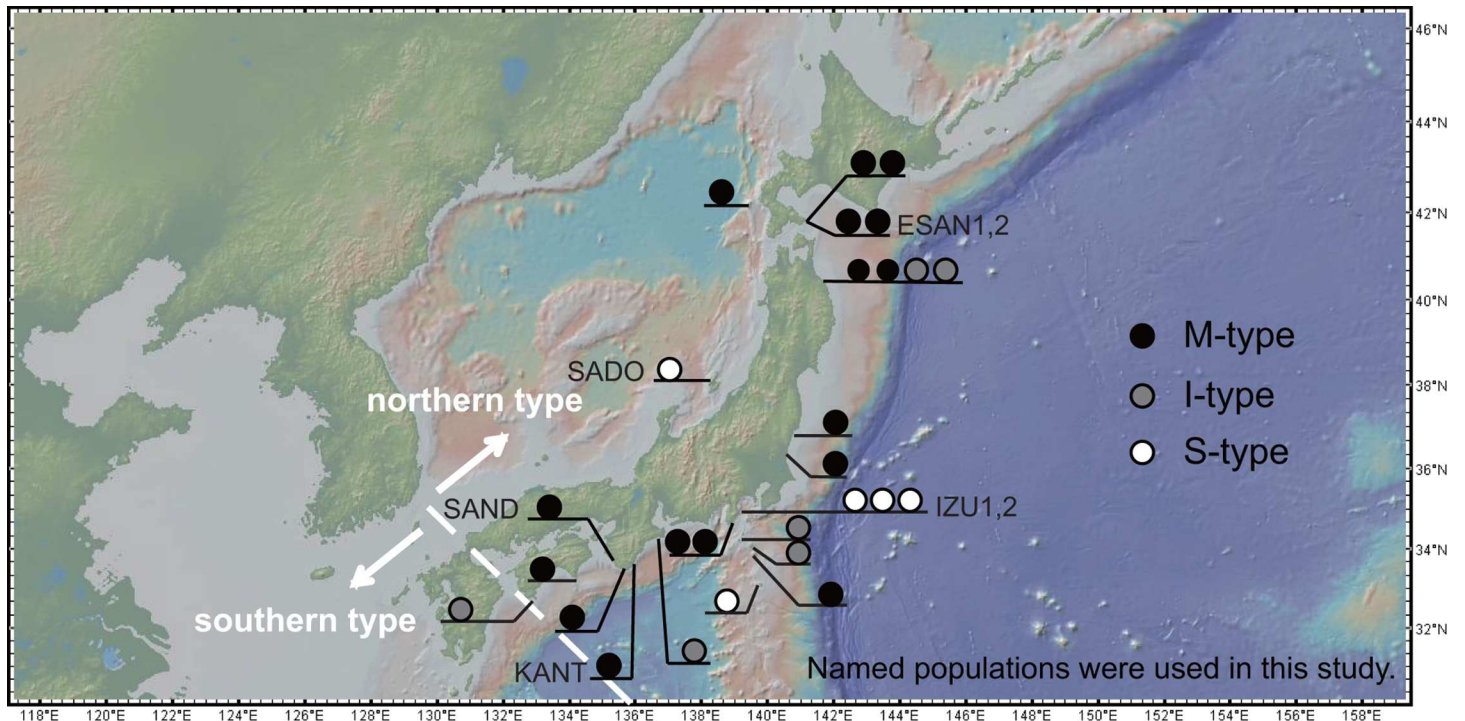
Fig 1. Distribution of northern and southern types of diploid sexual *Cyrtomiun falcatum* in Japan based on Matsumoto (2003) [11], and sampling locations of 7 populations examined in this study. Dashed line is the boundary of the northern and southern type's distributional range. This map was drawn by GeoMapApp (http://www.geomapapp.org/). Locations of the M-type (black circle), the I-type (gray circle) and the S-type (open circle) sporophyte individuals identified by Matsumoto (2003) [11] are shown.

doi:10.1371/journal.pone.0163683.g001

confirmed that all southern type individuals were the S-type. Traditionally, the S-type of gametangia formation on gametophytes (female at maturity) has been considered a morphological adaptation to promote outcrossing and the M-type (simultaneous hermaphrodite at maturity) enables gametophytic selfing [9,12]. In support of this hypothesis, gametophytes of the M-type sporophyte can produce sporophytes at very high rates (84%–100%) in isolated cultures, whereas the S-type sporophytes show a low rate of sporophyte formation (5%–35%) [11]. Ranker and Houston (2002) [13] compared the sexual expression of natural gametophytes with that of cultured gametophytes for the Hawaiian fern *Sadleria*, and suggested that the occurrence of simultaneously hermaphroditic (considered to be equivalent to the M-type) and unisexual gametophytes (S-type) in the laboratory would also be a good predictor of their occurrence in nature. Therefore, the S- and M-types observed in *C. falcatum* could be considered to reflect mating system variation in nature. Understanding this morphological variation is important because it helps clarify the role of mating systems in shaping genetic diversity of populations and may provide clues to the causes of mating system evolution. In the present study, we developed eight new microsatellite markers to evaluate genetic variation within and among populations of the northern type of *C. falcatum*. The specific aims of the present study were to: 1) test whether the wild populations of M-type individuals show higher selfing rates than those of the S-type individuals, 2) test correlations between high selfing rates, low genetic diversity and reduction of effective population size, if the selfing rate varies among populations, 3) estimate the past and current effective population size, and 4) test whether the M-type and the S-type populations are genetically differentiated.

Materials and Methods

Populations and sampling

The gametangia formation types, M-type or S-type, of the seven *C. falcatum* populations we examined are as determined by Matsumoto (2003) [11]. Briefly, Matsumoto (2003) [11] sowed spores on agar medium, and then transplanted each of the obtained gametophytes separately (e.g. one gametophyte in one separate well) onto vermiculite medium in the laboratory. At three months after spore sowing, forty gametophytes per sporophyte were examined to evaluate gametangia formation types [11]. Because each gametophyte was cultivated in isolation, variance in sexual expression by density [14] could be ignored. In Matsumoto's (2003) [11] experiment, 33 sporophyte individuals of the northern type of diploid *C. falcatum* from 20 localities (Fig 1) were examined.

For this study, we collected 233 sporophyte samples from seven populations (21–42 individuals per population) in five localities of sexual diploid populations of *C. falcatum* that were previously examined by Matsumoto (2003) [11]. The seven populations and their localities were as follows: ESAN 1 (41.8112N, 141.1844E) and ESAN 2 (41.8115N, 141.1844E) from Esan-misaki, Hokkaido Prefecture; SADO (38.0929N, 138.2498E) from Sado Island, Niigata Prefecture; IZU 1 (34.8824N, 139.1323E) and IZU 2 (34.8821N, 139.1319E) from Jogasaki, Shizuoka Prefecture; KANT (33.6004N, 135.6004E) from Kantori-misaki, Wakayama Prefecture; and SAND (33.6655N, 135.3355E) from Sandan-peki, Wakayama Prefecture (Fig 1). Three populations (IZU 1, IZU 2, SADO) were selected from the localities where the S-types have been observed, and four populations (ESAN 1, ESAN 2, SAND, KANT) were collected from the localities where M-types have been observed [11].

Voucher specimens of the samples (ri010001–ri010233) were deposited in the Herbarium of the National Museum of Nature and Science (TNS), Tsukuba, Ibaraki, Japan. For sampling in Esan Prefectural Natural Park, we obtained permission from the Hokkaido Government Biodiversity Division.

DNA extraction and microsatellite marker development

Total DNA was extracted from silica-dried leaves using the HEPES/CTAB method [15]. The DNA samples were used for microsatellite marker development and further genotyping. We developed microsatellite markers using two different methods; one was an improved technique for isolating co-dominant compound microsatellite markers [16] and the other was a next-generation sequencing (NGS) method [17].

Firstly, following the method of Lian *et al.* (2006) [16] genomic DNA of a sample from IZU1 was digested with six blunt-end cutters (*Hae*III, *Pvu*II, *Alu*I, *Ssp*I, *Eco*RI, and *Sca*I) and ligated with a specific blunt adaptor [18] using a T4 DNA Ligation kit (Nippon Gene, Tokyo, Japan). The digested and ligated fragments were amplified using a compound SSR primer $(AC)_5(AG)_8$ and an adaptor primer AP2 (5′-CTATAGGGCACGCGTGGT- 3′) [16]. The PCR products were cloned using the TOPO-TA Cloning Kit (Invitrogen, Carlsbad, USA). Plasmid DNAs were amplified from the colonies with a TemliPhi DNA Amplification Kit (GE Healthcare Bio-Sciences, Little Chalfont, UK). Sequence reactions were prepared with T3 and T7 primers (Invitrogen) using the BigDye Terminator v3.1 Cycle Sequencing Kit (Applied Biosystems, Tokyo, Japan). The reaction mixture was analyzed on an ABI 3500 genetic analyzer (Applied Biosystems). A total of 576 different fragments with a compound microsatellite motif at one end were obtained. From 86 different sequences, specific primers were designed and selected to have 200 to 400bp product length using PRIMER3 software [19]. A PIG1-tail (5'-GTTTCTT-3') was added to specific forward primers to reduce stuttering [20].

Secondly, we developed microsatellite markers using an NGS method with a Roche 454 Genome Sequencer Junior (Roche/454 Life Sciences, Branford, CT, USA). Genomic DNA was isolated from a pinna of the southern type of diploid *Cyrtomium falcatum*, collected from the Tsukuba Botanical Gardens (originally collected from Wakayama Pref., Japan) and fragmented by nebulization. A DNA library was constructed using the GS FLX Titanium Rapid Library Preparation Kit (Roche/454 Life Sciences). The DNA library was purified using the MinElute PCR Purification Kit (Qiagen, Tokyo, Japan) and its quality was checked using the Agilent High Sensitivity DNA kit (Agilent Technologies, Palo Alto, CA, USA). Emulsion PCR was carried out using the GS Junior Titanium emPCR Lib-L Kit (Roche/454 Life Sciences), and pyrosequencing was conducted on a Roche 454 Genome Sequencer Junior instrument at the Tsukuba Botanical Gardens, with the GS Junior Titanium Sequencing Kit (Roche/454 Life Sciences). Contigs were assembled to over 500bp with GS Newbler De Novo Assembler (Roche/454 Life Sciences), implementing the default parameters and heterozygotic mode. The program QDD v.2.1 [21] was used with default settings to detect and select microsatellite sequences. Twelve hundred contigs were used for searching microsatellite candidates. We designed 72 primer pairs based on the penalty scores calculated with Primer3 in the QDD pipeline. As described by Schuelke (2000) [22], the U19 sequence (5′-GGTTTTCCCAGTCACGACG-3′) was added to the 5′ end of specific forward primer sequences. A PIG2 tail (5'-GTTT-3') was added to specific reverse primer sequences [20].

Fragment analysis of microsatellite markers

We tested all of the candidate markers (86 by the method of Lian *et al.* (2006) [16] and 72 by the NGS method) for good PCR amplification, reproducibility, and the level of polymorphism over all samples, using a subset of samples: two individuals from each of the seven populations. Finally, eight primer pairs were selected and used to further genotype all samples (S1 Table). PCR amplifications (simplex PCR) were performed using the Multiplex PCR Kit (Qiagen) in a downscaled final volume of 5 µl according to the manufacturer's protocol. The forward and reverse primers were adjusted to 0.2 µM in final concentration and 20 ng of DNA was added to each reaction. For two primer sets, CFL-079 and CFL–C32, PCRs were conducted using each specific primer and a dye-labeled $(AC)_6(AG)_{10}$ primer (ABI PRISM®, Applied Biosystems) under the following conditions: initial denaturation for 15 min at 95°C, followed by 30 cycles at 95°C for 30 s, 55°C for 90 s, 72°C for 1 min, and final extension at 60°C for 30 min. The PCR reaction mixture for the other six primer sets contained 0.2 µM reverse primer, 0.04 µM forward primer, and 0.2 µM of the fluorescent dye-labeled U19 primer (ABI PRISM®, Applied Biosystems), which acted as the second forward primer for the cycles following the touchdown stage. Touchdown PCR was performed with initial denaturation for 15 min at 95°C, followed by 25 cycles at 95°C for 30 s, 63–53°C (with a 0.5°C decrease for every subsequent cycle) for 90 s, and 72°C for 1 min, followed by 20 cycles of 95°C for 30 s, 53°C for 90 s, and 72°C for 1 min, and final extension at 60°C for 30 min. The PCR products were analyzed on an ABI 3500 Genetic Analyzer (Applied Biosystems) with the internal size standard, GeneScan 600 LIZ (Applied Biosystems), and fragment sizes were determined with GeneMapper 3.1 (Applied Biosystems). The original sequences for the markers were deposited in GenBank under the accession numbers LC055975—LC055982 (S1 Table).

Data analyses

Inbreeding coefficient and genetic diversity within populations. Gene diversity (h; [23]) and allelic richness (A_R; [24]) were calculated for each population using FSTAT ver. 2.9.3.2 [25]. FSTAT was also used to test genotypic disequilibrium among loci for each population.

We used INEST2 [26], with the 'nfb' model, to estimate F_{IS} values within populations, taking into account the effect of underestimating heterozygosity in the presence of null alleles. As mentioned previously, two types of self-fertilization may occur in homosporous ferns: gametophytic (S_I) and sporophytic (S) selfing. Hedrick (1987) [27] derived a formula showing the relationship among F_{IS} and the rates of two types of selfing (S_I and S).

$$F_{IS} = \frac{S + 2S_I}{2 - S}$$

In the present study, we use F_{IS} values as an indicator of the relative contributions of selfing *sensu-lato* (both S and S_I) to outcrossing [28]. To assess whether population genetic parameters differ between M- and S-type populations, inbreeding coefficients (F_{IS}), gene diversity (h), allelic richness (A_R), relatedness [29], and F_{ST} [30] values were calculated and compared, treating M- and S-types as two groups. Differences in these values between the two types were tested for significance using a randomization test in FSTAT. We employed one-sided *P*-values to test whether the value in one group is significantly larger than the other. Our STRUCTURE analysis (see below) indicated that cluster 6 at $K = 6$ was admixed in both SAND and SADO populations, although these two populations are located far apart from each other (Fig 1, see Results and Discussion for details). This cluster 6 was further divided into two clusters in $K = 7$ corresponding to each of the two populations. As we found that these admixed clusters affected the evaluation of genetic diversity in these two populations, we also analyzed genetic diversity in the two populations after removing individuals which had ancestry values of greater than 50% to cluster 6 in $K = 6$.

Genetic differentiation and structure among populations.   Genetic differentiation among populations was evaluated by calculating the overall and pairwise F_{ST} [30] values and their respective confidence intervals (95%) were determined on the basis of 1000 bootstrapping replicates using FSTAT. The standardized values of F_{ST} and F'_{ST} [31] were also calculated using GenAlEx 6.5 [32]. Patterns of isolation by distance (IBD; [33]) were evaluated, using GenAlEx [32], according to the method described by Rousset (1997) [34]; a Mantel test (with 999 random permutations) between the matrices obtained for pairwise population differentiation in terms of $F_{ST}/(1-F_{ST})$ and the natural logarithms of direct minimum geographic distance among populations. Genetic structure was also investigated with the model-based clustering algorithm implemented in the software STRUCTURE v. 2.3.3 [35,36]. A number of clusters (K) varying from 1 to 15, were evaluated under the correlated allele frequencies model by running 100,000 burn-in Markov Chain Monte Carlo (MCMC) repetitions and 1,000,000 subsequent repetitions based on the LOCPRIOR model [36]. The probabilities of each K were averaged over 10 runs. We employed the CLUMPAK server [37] to evaluate multimodality [38] among runs at each K. The optimum K value was determined based on ΔK [39], evaluating the probability of the data (Ln P(D)) for each K value using STRUCTURE HARVESTER [40]. Bar charts representing the proportion of cluster membership in each individual were obtained using CLUMPAK. The genetic relationships between the clusters were evaluated based on genetic distance calculated in STRUCTURE and a neighbor-joining tree of clusters was generated using Populations 1.2.23 [41].

Inference of past population size change and effective population size.   The software DIYABC v2.0 [42,43] was used to infer past population size changes and the effective population size of *Cyrtomium falcatum* based on the Approximate Bayesian Computation (ABC) approach. DIYABC provides flexibility for the mutation models of microsatellite loci in coalescent simulations, allowing both the generalized stepwise mutation model (GSM; [44]) and the single nucleotide indel model (SNI). As our main purpose was to test whether the effective population size and demographic history among M- and S-type populations were different due to

their different forms of gametangia formation, three simple scenarios were examined in each population (S1 Fig):

Scenario 1. Bottleneck model: the ancestral effective population size (N_a) was changed at t_1 to the modern effective population size (N_1) and N_1 was set to be smaller than N_a.

Scenario 2. Constant model: the ancestral effective population size (N_b) and the modern one (N_1) were set to be equal, assuming the effective population size has not changed.

Scenario 3. Expansion model: the ancestral effective population size (N_c) was changed at t_1 to the modern effective population size (N_1) and N_1 was set to be larger than N_c.

In these scenarios, t_1 represents time scale measured by generation time. We employed the default values of the priors for each parameter in DIYABC. The mean values for expected heterozygosity (H_E), number of alleles (A), allele size variance across loci and M index across loci [45,46] were used as summary statistics. A million simulations were run for each scenario. After all the simulations had been run, the most-likely scenario was determined by comparing the posterior probabilities using the logistic regression method. The goodness of fit of the scenario was assessed by the option "model checking" with principal component analysis (PCA) in DIYABC, which measures the discrepancy between the model and real data. To translate the inferred number of generations for t_1 to time scale by year, we assumed a generation time of 3 years, as Matsumoto (2003) [11] showed that the northern type of *C. falcatum* produces spores at 1 year in cultivation tests.

Results

Characteristics of the eight microsatellite loci

Eight new microsatellite markers were developed in this study (S1 Table). The number of detected alleles ranged from 2 (locus CFL-B16) to 14 (locus CFL-B-02 and CFL-079) and a total of 64 alleles were detected across all 8 loci (S2 Table). The null allele frequencies estimated by INEST2 (S3 Table) were relatively high (over 0.10) in 9 out of 56 (8 loci × 7 populations) combinations, but significant in only one case: CFL-B12 locus in SADO (0.246; 95% CI: 0.0977–0.400). No significant deviations from genotypic equilibrium were detected once putative admixed individuals in SADO were excluded.

Mating system and genetic diversity

All of the populations, except for SADO, showed significantly positive inbreeding coefficient (F_{IS}) values, ranging from 0.220 to 0.794 over all loci (Table 1). The average F_{IS} value of M-type populations (0.626) was significantly higher than S-type (0.208, $P < 0.05$; Table 2). The F_{IS} values estimated using INEST2 (S4 Table) did not largely differ from those of FSTAT, suggesting that the presence of null alleles had little influence on the overall results. The average allelic richness (A_R) of the M-type populations (1.999) was significantly lower than that of the S-type populations (2.718, $P < 0.05$; Table 2). Similarly, the average value of gene diversity (h) of the M-type populations (0.152) was significantly lower than that of the S-type populations (0.367, $P < 0.05$; Table 2). When admixed individuals were included in these analyses, different trends were not detected (Table 2).

Population genetic structure

The overall F_{ST} and F'_{ST} values were 0.581 and 0.739, respectively, indicating a high level of genetic differentiation among populations. This pattern was not changed when admixed individuals were removed from the data ($F_{ST} = 0.521$, $F'_{ST} = 0.699$). The average of the pairwise F_{ST} values among the M-type populations was higher than that among the S-type populations, and

Table 1. Genetic diversity indices and inbreeding coefficient values for seven populations of the northern type of diploid *Cyrtomium falcatum*.

	M-type populations				S-type populations		
	ESAN1	**ESAN2**	**SAND**	**KANT**	**IZU1**	**IZU2**	**SADO**
N_A	2.130	2.125	2.500 (3.750)	2.250	3.750	2.625	3.000 (4.125)
A_R	1.700	1.847	2.380 (3.626)	2.074	2.900	2.390	2.863 (3.776)
h	0.076	0.158	0.227 (0.374)	0.217	0.378	0.326	0.436 (0.562)
F_{IS}	**0.501**	**0.671**	**0.794 (0.602)**	**0.560**	**0.340**	**0.220**	-0.100 **(0.157)**
N_1	169	210	299	328	846	465	715

N_A, mean number of alleles; A_R, allelic richness; h, gene diversity; F_{IS}, multilocus estimate of inbreeding coefficient; N_1, current effective population size estimated by DIYABC. Bold type indicates significant F_{IS} values ($p < 0.00089$, simple Bonferroni correction for 5% level). Genetic diversity indices and inbreeding coefficient values in parentheses are those calculated for all samples including the admixed individuals revealed by the STRUCTURE analysis.

doi:10.1371/journal.pone.0163683.t001

the difference was nearly significant ($P = 0.067$). Significant IBD was detected among the 7 populations, both with ($R^2 = 0.3447$; $P < 0.05$) and without ($R^2 = 0.3435$; $P < 0.05$) the admixed individuals included (Fig 2). In the STRUCTURE analysis, the mean probability of the data (LnP(D)) increased steadily up to $K = 7$ (S2 Fig) and ΔK suggested $K = 7$ as optimal (S2 Fig). At $K = 2$, ESAN 1 and 2 were grouped into cluster 1 and the remaining populations were assigned to cluster 2 (Fig 3). Thus, the clustering at $K = 2$ did not correspond to the M- and S-types. At $K = 3$, two M-type populations (KANT and SAND) in Wakayama Prefecture and one S-type population (SADO) were separated from IZU1 and IZU2. At $K = 4$, KANT was differentiated. At $K = 5$ and greater, five clusters corresponding to the five main sampling localities (Fig 1) were observed. At $K = 6$, SADO and SAND populations were shown to contain a considerable number of admixed individuals (with cluster 6). At $K = 7$, cluster 6 was further divided into two clusters and cluster 7 corresponded to the admixed cluster in SAND. The NJ tree for the seven clusters revealed two groups. In one group, cluster 1 (ESAN 1 and 2), 2 (IZU 1 and 2), 4 (KANT) and 5 (major cluster in SAND) were grouped together, while cluster 3 and 6 in SADO and cluster 7 for the admixed cluster in SAND were in the other group. The F values of each cluster (analogous to the F_{ST} values between each cluster and the assumed ancestral population) showed that clusters corresponding to M-type populations had larger values (0.627–0.751) than S-type populations (0.474–0.508, Fig 3).

Table 2. Group comparison of population genetic parameters between the M- and the S-type populations of the northern type of diploid *Cyrtomium falcatum*.

	A_R	h	F_{IS}	Relatedness	F_{ST}
M-type	1.999	0.152	0.626	0.708	0.663
(all samples)	(2.378)	(0.177)	(0.587)	(0.672)	(0.619)
S-type	2.718	0.367	0.208	0.490	0.367
(all samples)	(3.110)	(0.410)	(0.241)	(0.440)	(0.328)
P-value (M>S)	0.989	1.000	0.029*	0.064	0.067
(all samples)	(0.890)	(0.977)	(0.002*)	(0.560)	(0.270)
P-value (S>M)	0.016*	0.009*	0.981	0.963	0.967
(all samples)	(0.168)	(0.053)	(1.000)	(0.954)	(1.000)

A_R, allelic richness; h, gene diversity; F_{IS}, multilocus estimate of inbreeding coefficient; F_{ST}, pairwise F_{ST} value among populations
*, P-values less than 0.05. Population genetic parameters calculated using all samples including the admixed individuals revealed by the STRUCTURE analysis are shown in parentheses.
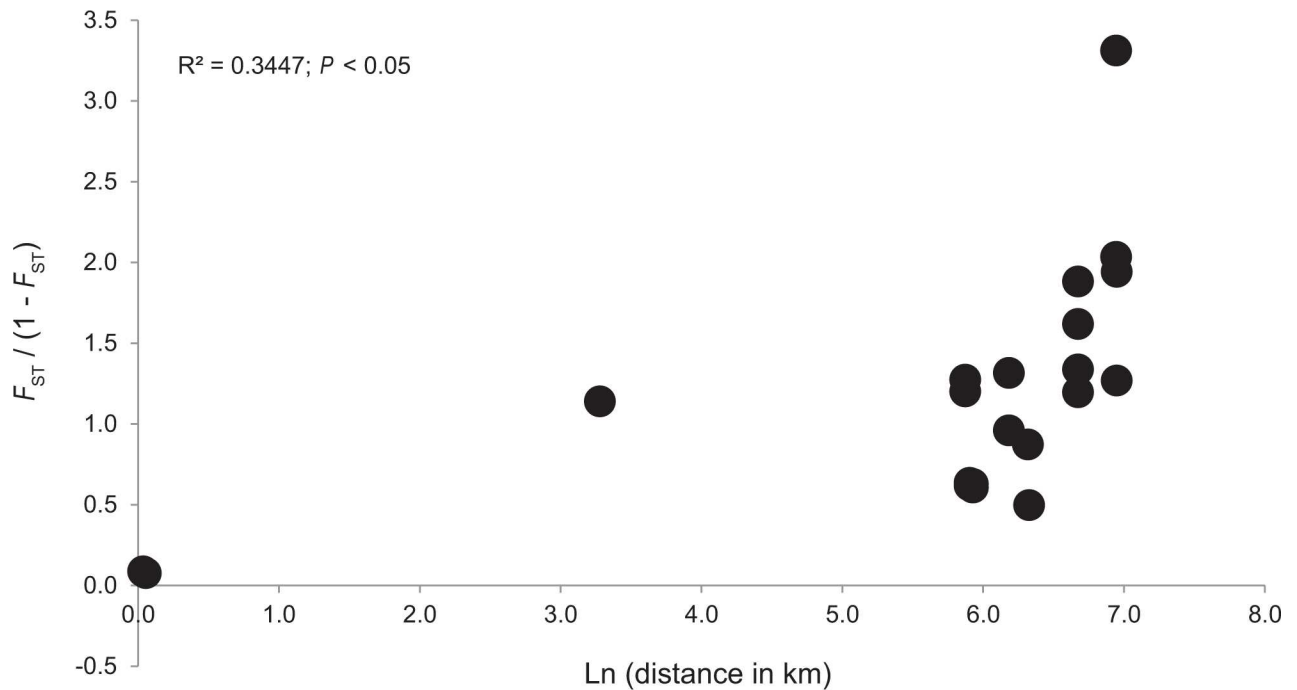
doi:10.1371/journal.pone.0163683.t002

Fig 2. Isolation by distance for the 7 populations of the northern type of diploid *Cyrtomium falcatum*. The relationship between the matrix of pairwise differentiation described as $F_{ST} / (1 - F_{ST})$ and the matrix of the natural logarithm of geographic distance (in meters) among the 7 populations.

doi:10.1371/journal.pone.0163683.g002

Inference of demographic history of each population

In DIYABC, the highest posterior probability was for scenario 1 (bottleneck model), and its 95% confidence interval (CI) did not overlap with those of the other two scenarios in each of the 7 populations, regardless of gametangia formation type (S5 Table). For scenario 1, the median values of the effective modern population size of N_1 were well estimated in each population. The S-type populations had significantly larger N_1 values (465–846) than the M-type ones (169–328; t-test, $P < 0.05$). However, the posterior distribution pattern suggested that other parameters were poorly estimated (S3 Fig and S6 Table), with the exception of the timing of the population size change event (t_1) in the SADO population. In the SADO population, the median value of t_1 was 2,940 generations ago (95% CI, 256–9,390), corresponding to 8,820 years ago (95% CI, 768–28,170). In all populations, all of the summary statistics showed no significant differences between the observed and simulated data, based on the posterior distributions (S6 Table), and the PCA showed that the observed data point was centered on the cluster of simulated data points, based on the posterior distributions (S4 Fig), suggesting that scenario 1 was a good fit to the observed data in all populations.

Discussion

Mating system differentiation, genetic diversity and effective population size

We found evidence for mixed mating in the northern type of diploid *C. falcatum*, as all but one population (SADO) had significantly positive F_{IS} values, ranging from 0.2 to 0.8, indicating it is highly likely that gametophytic selfing, sporophytic selfing, and outcrossing are all occurring in these populations. In contrast to our results, Chung et al. (2012) [47] examined sexual *C.*
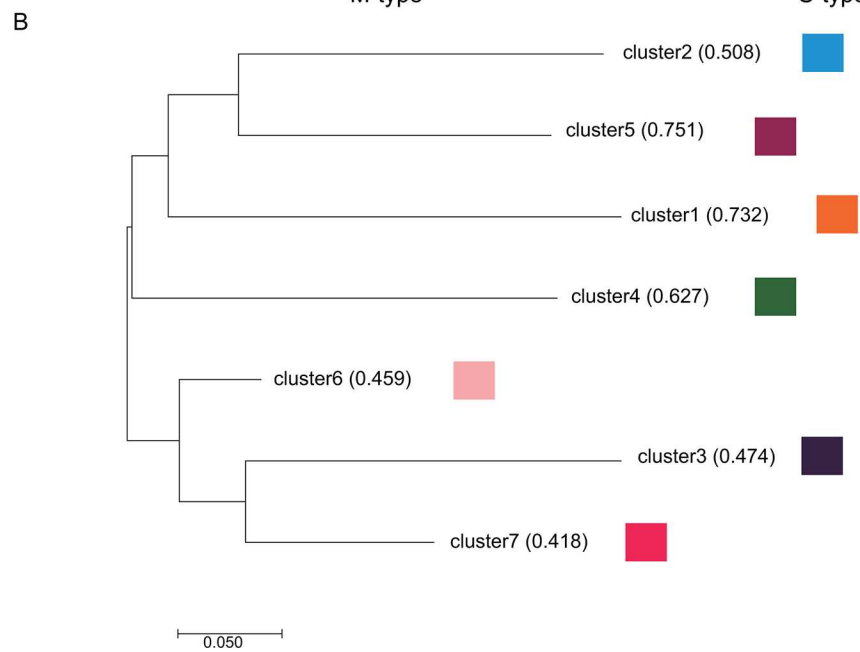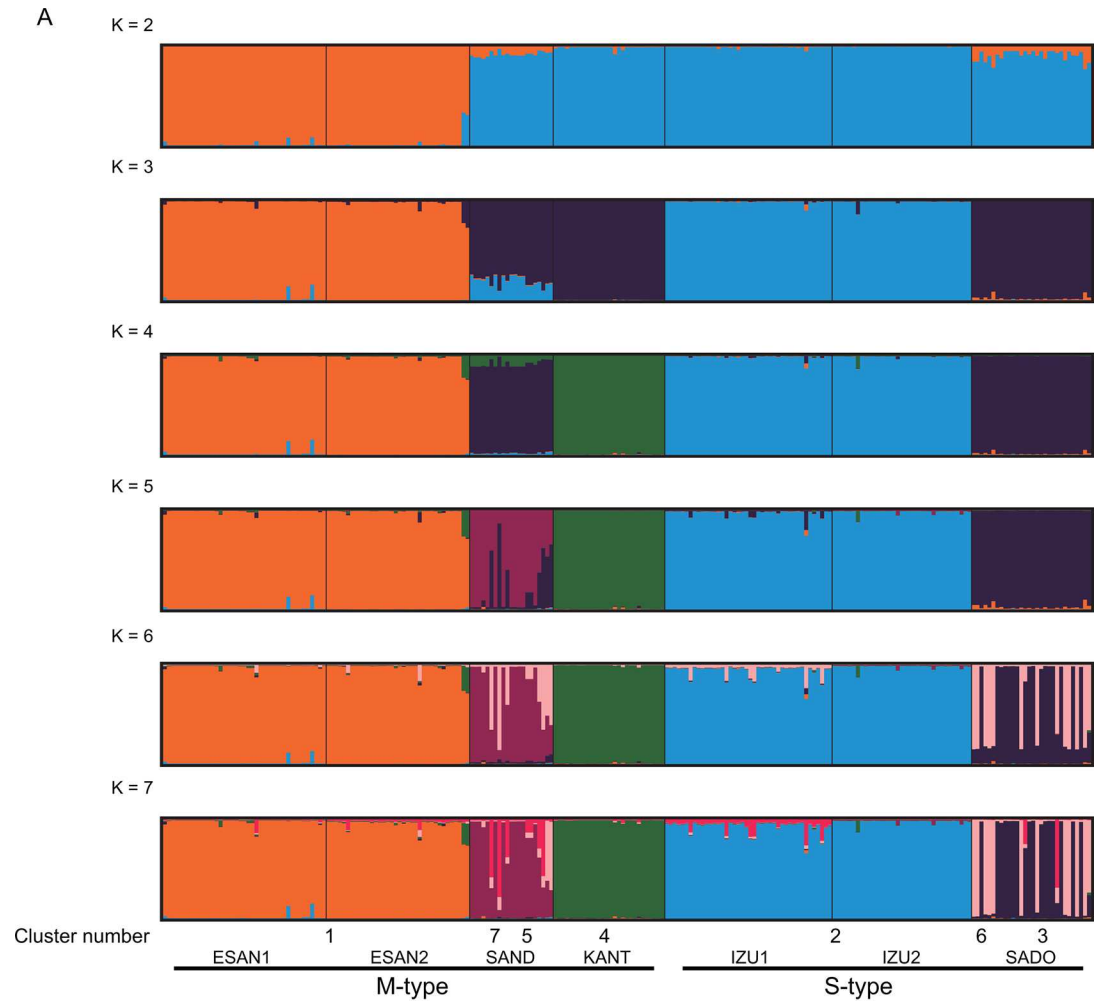
Fig 3. Results of the STRUCTURE analysis and the Neighbor-joining (NJ) tree of the clusters when _K_ = 7. (A) The proportion of the membership coefficient of 233 individuals in the 7 populations for each of the inferred clusters for _K_ = 2–7 defined using Bayesian clustering in STRUCTURE analysis. Population types and cluster numbers on the NJ tree are indicated under the plot of _K_ = 7. (B) The NJ tree of the seven clusters for _K_ = 7. Values shown next to each cluster number are F_{ST} values between each cluster and the common ancestral population.

falcatum populations along the southern shores of South Korea, and showed that the F_{IS} values for these populations did not significantly deviate from zero, suggesting the prevalence of outcrossing. The _C. falcatum_ individuals described in Chung et al. (2012) [47] may be the southern type, because Matsumoto (2003) [11] reported the distribution of the southern type in Nagasaki Pref., Japan (Fig 1), which is only 200 km away from southern South Korea, separated by the Tsushima Strait. Matsumoto (2003) [11] suggested that the southern type was an outcrosser based on its S-type of sexual expression of gametophytes, and the consistently low rates of sporophyte formation in isolated cultures. Because of the existence of these different mating systems, the two sexual diploid _C. falcatum_ types provide an interesting experimental opportunity for future evolutionary studies pertaining to the transition between obligate outcrossing and mixed mating in homosporous ferns.

A cluster specific to the SADO and SAND populations, which are located far apart from one another, was detected in the STRUCTURE analysis (_K_ = 6, cluster 6, Fig 3). One of the possible explanations for this cluster is long-distance dispersal of the southern type into the northern range followed by hybridization of the northern and southern types. Although we examined voucher specimens of SADO and SAND populations, there were no morphological differences between the pure and admixed individuals revealed in the STRUCTURE analysis. Additional studies including samples of the southern type are required to clarify the geographical distribution pattern of the two types of _C. falcatum_.

The F_{IS} values of M-type populations were significantly higher than those of S-type ones (Tables 1 and 2). Allelic richness (A_R) and gene diversity (h) values of M-type populations were lower than those of S-type ones and the effective population size estimated by DIYABC also showed the same pattern (Tables 1 and 2). We acknowledge that there are several sources of uncertainty and assumptions in the ABC approach (e.g. assumptions about the generation time, overlapping generations, confidence intervals of the estimated parameters and the assumed model; for details see Tsuda et al. (2015) [48]). DIYABC does not assume gene flow after divergence, which may bias estimates of divergence time and effective population size when demographic scenarios for multiple samples (e.g. population, species) are examined [48,49]. For this reason, we did not include population splits in our scenarios and only inferred the temporal effective population size change in single populations. Moreover, the relatively high F'_{ST} value suggests that gene flow among populations might be restricted. Thus, although we need to consider the assumptions of the methods used in genetic analyses, we believe the results of ABC are informative regarding the differences between the two types of populations in our study. Indeed, although the inference of effective population size change in single populations is a simple ABC approach, Sakaguchi et al. (2013) [50] employed a similar approach to successfully detect geographic patterns in effective population size of conifer species in Australia.

To our knowledge, this is the first study to show that the type of gametangia formation of gametophytes affects the levels of inbreeding and genetic diversity in natural populations of homosporous ferns. It is well known that inbreeding species have lower neutral genetic diversity within populations compared to outcrossing taxa [51]. The correlation between genetic diversity and gametangia formation in M- and S-types of _C. falcatum_ follows these general trends. The observed patterns could be due to several factors. Firstly, inbreeding is expected to

reduce effective population size: $N_e = N / (1+F_{IS})$ [52]. Secondly, recent empirical studies in seed plants have revealed that reduction of genetic diversity or effective population size are often greater than those expected from F_{IS} values alone [8], possibly because of linked selection owing to reduced recombination efficiency [53], and/or because of population bottlenecks. In the present study, despite their intermediate F_{IS}, average gene diversity (h) of the M-type populations (0.152) was about half that of S-type populations (0.367), and the average N_e of the M-type populations (215) was about a third of that of S-type populations (675). Although the 95% CIs of the inferred N_e values in the ABC should be taken into consideration, these levels of reduction in h and N_e are comparable to the case of complete inbreeding, and seem to be greater than those expected from the intermediate F_{IS} values observed in M- and S-type populations (0.626 vs. 0.208). One possible explanation for population bottlenecks is colonization. The gametophytic selfing in ferns is hypothesized to be an advantage for long-distance colonization, as it enables a single spore to establish a new population [4,54,55]. For example, de Groot et al. (2012) [56] examined fern populations in a recently reclaimed Dutch polder land and concluded that the polder land was colonized via multiple independent single-spore colonization events in all four species studied. It is likely that simultaneous formation of both male and female gametangia and higher rates of selfing confer higher colonization ability to M-type individuals. This selfing ability is likely to be advantageous for range expansion and also following colonization. Both M- and S-type individuals of the northern type are lithophytes that grow on sea cliffs, a habitat that is vulnerable to disasters such as landslides. In fact, one population of the northern type in Fukushima Pref. was lost after the 2011 Great East Japan Earthquake and Tsunami [57]. DIYABC detected past population bottlenecks (Scenario 1, S1 Fig) in all populations regardless of M- or S-type (S4 Table), and this might reflect past episodes of local extinction and recolonization in unstable habitats. Although there is no apparent difference between the habitats of M- and S-types, it is possible that differences in magnitude or frequency of past colonization bottleneck events could result in significant differences in the F_{ST}, genetic diversity and effective population sizes between M- and S-type populations.

Population genetic structure

Previous studies using allozymes or microsatellites showed that the standardized F'_{ST} values are strongly variable in homosporous fern species (as they are in seed plant species), e.g. $F'_{ST} = 0.068$ for *Odontosoria chinensis* in Hawaii [58], $F'_{ST} = 0.761$ for *Dryopteris aemura* in Spain [59], $F'_{ST} = 0.589$ for *Cyrtomium falcatum* in Korea [47], and $F'_{ST} = 0.414$ for *Selliguea hastata* in Japan [60] (all F'_{ST} values calculated by R.I.). The F'_{ST} values (0.739) of the present study are relatively high. Interestingly, Korean outcrossing populations of *C. falcatum* [47] also have a relatively high overall F'_{ST} value (0.589) when compared to the northern type of *C. falcatum*, despite their putative outcrossing. This may indicate that this level of population differentiation is typical for the species and could be due to species dispersal ability and/or habitat preferences. For example, it is possible that a discontinuous geographical distribution of suitable habitat, such as crevices in sea cliffs or rocks near the seashore, is responsible for population differentiation. Significant IBD was detected in this study (Fig 2) and the STRUCTURE analysis did not show clear clustering corresponding to the M- and S-type populations (Fig 3). Although more populations would be required to conclude, we suggest that range-wide genetic structure of this species is not generated by M- and S-type differences, but rather by dispersal limitation. Significant IBD, related to past range shifts following climate change, has been detected in many plant species in the Japanese archipelago [61–63]. Significant IBD was also reported in a fern species, *Asplenium fontanum* subsp. *fontanum*, in Europe [64] and was likely caused by range expansion following the last glacial maximum (LGM). Similarly, past range shift in

relation to the LGM was described in *Selliguea hastata* in Korea and Japan [60]. Although not well examined in palaeoecological studies of spore fossils, past distributional shifts in relation to the LGM might play an important role in generating the modern genetic structure of *C. falcatum*. Interestingly, although the time scale of population size change in the northern type of *C. falcatum* was well estimated in only one population (SADO, 8820 years ago, 95%CI: 1224–26610 years ago), this timing corresponds to a post-LGM recolonization scenario.

The M- and S-types of *C. falcatum* were significantly different in levels of selfing (F_{IS}), genetic diversity, and effective population size. These results suggest that reproductive and demographic differences exist between the two types, despite the lack of genetic structure between them. The more severe population bottlenecks were inferred to have occurred in the M-type populations rather than the S-types. This implies that local extinction and recolonization events could provide opportunities for the maintenance of the M-type populations, and possibly for increasing the frequency of the M-type individual in some cases, even under occasional immigration of the S-type individuals. Evolution of selfing via transmission advantage operates only under a low genetic load, and fixed selfing is expected [7]. Therefore, the existence of mixed mating even in the M-type populations would suggest that reproductive assurance, rather than transmission advantage, is the main factor affecting the evolution of selfing in this species. If this is the case, the M-type would be advantageous in small and disturbed populations, while the S-type would be advantageous in large and stable populations.

In this study, we discuss results obtained after removing putative admixed individuals in SADO and SAND populations. Subpopulation genetic structure within these two populations may be one of the reasons why a clearer difference in genetic diversity between the S- and M-types was detected only after the removing admixed samples. However, it is difficult to discuss the origin of cluster 6 and 7 in detail with the current dataset. One possible explanation is migration and hybridization of northern and southern types of *C. falcatum* in these areas, although this was not expected given the morphological observations of Matsumoto 2003 [11]. However, our on-going study based on restriction site associated DNA sequencing (RAD-seq) supports this hypothesis (Imai et al. unpublished). We would need to sample individuals covering the species entire distributional range, including both southern and northern types, and evaluate genetic variation using several types of markers to clarify sympatric distribution and hybridization.

Supporting Information

S1 Fig. Demographic models used in DIYABC for each population of *C. falcatum*. Scenario 1. Bottleneck model: the ancestral effective population size (N_a) was changed at t_1 to the modern effective population size (N_1) and N_1 was set to be smaller than N_a Scenario 2. Constant model: the ancestral effective population size (N_b) and the modern one (N_1) were set to be equal, assuming the effective population size has not changed. Scenario 3. Expansion model: the ancestral effective population size (N_c) was changed at t_1 to the modern effective population size (N_1) and N_1 was set to be larger than N_c.
(EPS)

S2 Fig. The values of posterior probability of the data (Ln P(D)) from 10 runs for each value of K (1–15; A) and ΔK (right B).
(EPS)

S3 Fig. Prior and posterior distributions for each parameter obtained by DIYABC analysis for each population. X axis indicates values for the parameter described in the title of each graph; pmic: the parameter of the geometric distribution to generate multiple stepwise

mutations; smic: Mean mutation rate of single nucleotide indel; μmic: mean mutation rate of SSR. Y axis indicates probability of prior and posterior.
(PPTX)

S4 Fig. Principal Component Analysis (PCA) score plot obtained from DIYABC analysis for each population. PCA plots of prior, posterior and observed data set for summary statistics.
(PPTX)

S1 Table. Primer sequences, repeat motifs, and accession numbers of source sequences for eight microsatellite markers developed in this study.
(DOCX)

S2 Table. Genetic diversity indices and inbreeding coefficient values for seven populations of diploid *Cyrtomium falcatum*.
(DOCX)

S3 Table. Null allele frequencies at each locus estimated by INEST2.
(DOC)

S4 Table. Inbreeding coefficient (F_{IS}) values estimated by INEST2 for seven populations of the northern type of diploid *Cyrtomium falcatum*.
(DOCX)

S5 Table. Posterior probability of each scenario by DIYABC.
(XLSX)

S6 Table. Demographic parameters of scenario 1 obtained by DIYABC.
(XLSX)

S7 Table. Genotype list of all samples.
(XLSX)

Acknowledgments

Author Contributions

Conceptualization: RI YT SM YW.

Formal analysis: RI YT.

Funding acquisition: YW.

Methodology: RI YT YW.

Resources: RI SM AE YW.

Software: RI YT.

Supervision: YW.

Writing – original draft: RI YT YW.

Writing – review & editing: RI YT AE YW.

References

1. Yampolsky C, Yampolsky H. Distribution of sex forms in the phanerogamic flora. Bibl Genet. 1922; 3: 1–62.

2. Busch JW, Delph LF. The relative importance of reproductive assurance and automatic selection as hypotheses for the evolution of self-fertilization. Ann Bot. 2012; 109: 553–562. doi: 10.1093/aob/mcr219 PMID: 21937484

3. Fisher R. Average excess and average effect of a gene substitution. Ann Eugenic. 1941; 11: 53–63. doi: 10.1111/j.1469-1809.1941.tb02272.x

4. Baker HG. Self-compatibility and establishment after "long-distance" dispersal. Evolution. 1955; 9: 347–9. doi: 10.2307/2405656

5. Morgan MT, Wilson WG. Self-fertilization and the escape from pollen limitation in variable pollination environments. Evolution. 2005; 59: 1143–1148. doi: 10.1554/04-422 PMID: 16136811

6. Darwin C. The effects of cross and self fertilisation in the vegetable kingdom. London: John Murray; 1876.

7. Lande R, Schemske DW. The evolution of self-fertilization and inbreeding depression in plants. I. genetic models. Evolution. 1985; 39: 24–40. doi: 10.2307/2408514

8. Shimizu KK, Tsuchimatsu T. Evolution of selfing: recurrent patterns in molecular adaptation. Annu Rev Ecol Evol Syst. 2015; 46: 593–622. doi: 10.1146/annurev-ecolsys-112414-054249

9. Klekowski EJ. Reproductive biology of the Pteridophyta. II. Theoretical considerations. Bot J Linn Soc. 1969; 62: 347–359. doi: 10.1111/j.1095-8339.1969.tb01972.x

10. Sessa EB, Testo WL, Watkins JE. On the widespread capacity for, and functional significance of, extreme inbreeding in ferns. New Phytol. 2016; 211: 1108–1119 doi: 10.1111/nph.13985 PMID: 27094807

11. Matsumoto S. Species ecological study on reproductive systems and speciation of *Cyrtomium falcatum* complex (Dryopteridaceae) in Japanese archipelago. Ann Tsukuba Bot Gard. 2003; 22: 1–141.

12. Masuyama S. The sequence of the gametangium formation in homosporans fern gametophytes: 1. Patterns and their possible effect on the fertilization, with special reference to the gametophytes of *Athyrium*. Sci Rep Tokyo Kyoiku Daigaku, B. 1975; 16: 47–69.

13. Ranker TA, Houston HA. Is gametophyte sexuality in the laboratory a good predictor of sexuality in nature? Am Fern J. 2002; 92: 112–118. doi: 10.1640/0002-8444(2002)092[0112:igsitl]2.0.co;2

14. Huang Y, Chou H, Chiou W. Density affects gametophyte growth and sexual expression of *Osmunda cinnamomea* (Osmundaceae: Pteridophyta). Ann Bot. 2004; 94: 229–232. doi: 10.1093/aob/mch142 PMID: 15229126

15. Shepherd LD, McLay TGB. Two micro-scale protocols for the isolation of DNA from polysaccharide-rich plant tissue. J Plant Res. 2011; 124: 311–314. doi: 10.1007/s10265-010-0379-5 PMID: 20927638

16. Lian CL, Wadud MA, Geng Q, Shimatani K, Hogetsu T. An improved technique for isolating codominant microsatellite markers. J Plant Res. 2006; 119: 415–417. doi: 10.1007/s10265-006-0274-2 PMID: 16636745

17. Takayama K, Patricio LS, König C, Kohl G, Novak J, Stuessy TF. A simple and cost-effective approach for microsatellite isolation in non-model plant species using small-scale 454 pyrosequencing. Taxon. 2011; 60: 1442–1449.

18. Lian C, Zhou Z, Hogetsu T. A simple method for developing microsatellite markers using amplified fragments of inter-simple sequence repeat (ISSR). J Plant Res. 2001; 114: 381–385. doi: 10.1007/pl00014001

19. Rozen S, Skaletsky H. Primer3 on the WWW for general users and for biologist programmers. Methods Mol Biol. 2000; 132: 365–386. doi: 10.1385/1-59259-192-2:365 PMID: 10547847

20. Brownstein MJ, Carpten JD, Smith JR. Modulation of non-templated nucleotide addition by Taq DNA polymerase: primer modifications that facilitate genotyping. Biotechniques. 1996; 20: 1004–1006. PMID: 8780871

21. Meglécz E, Costedoat C, Dubut V, Gilles A, Malausa T, Pech N, et al. QDD: A user-friendly program to select microsatellite markers and design primers from large sequencing projects. Bioinformatics. 2009; 26: 403–404. doi: 10.1093/bioinformatics/btp670 PMID: 20007741

22. Schuelke M. An economic method for the fluorescent labeling of PCR fragments. Nat Biotechnol. 2000; 18: 233–234. doi: 10.1038/72708 PMID: 10657137

23. Nei M. Molecular evolutionary genetics. New York: Columbia university press; 1987.

24. El-Mousadik A, Petit RJ. High level of genetic differentiation for allelic richness among populations of the argan tree [*Argania spinosa* (L.) Skeels] endemic to Morocco. Theor Appl Genet. 1996; 92: 832–839. doi: 10.1007/BF00221895 PMID: 24166548

25. Goudet J. FSTAT, a program to estimate and test gene diversities and fixation indices (version 2.9. 3). 2001. Available: http://www2.unil.ch/popgen/softwares/fstat.htm.

26. Chybicki IJ, Burczyk J. Simultaneous estimation of null alleles and inbreeding coefficients. J Hered. 2009; 100: 106–113. doi: 10.1093/jhered/esn088 PMID: 18936113

27. Hedrick PW. Genetic load and the mating system in homosporous ferns. Evolution. 1987; 41: 1282–1289. doi: 10.2307/2409093

28. Soltis PS, Soltis DE. Evolution of inbreeding and outcrossing in ferns and fern-allies. Plant Species Biol. 1990; 5: 1–11. doi: 10.1111/j.1442-1984.1990.tb00187.x

29. David C. Queller KFG. Estimating relatedness using genetic markers. Evolution. 1989; 43: 258–275. doi: 10.2307/2409206

30. Weir BS, Cockerham CC. Estimating F-statistics for the analysis of population structure. Evolution. 1984; 38: 1358–1370. doi: 10.2307/2408641

31. Meirmans PG, Hedrick PW. Assessing population structure: F_{ST} and related measures. Mol Ecol Resour. 2011; 11: 5–18. doi: 10.1111/j.1755-0998.2010.02927.x PMID: 21429096

32. Peakall R, Smouse PE. GenAlEx 6.5: genetic analysis in Excel. Population genetic software for teaching and research-an update. Bioinformatics. 2012; 28: 2537–2539. doi: 10.1093/bioinformatics/bts460 PMID: 22820204

33. Wright S. Isolation by distance. Genetics. 1943; 28: 114–138. PMID: 17247074

34. Rousset F. Genetic differentiation and estimation of gene flow from F-statistics under isolation by distance. Genetics. 1997; 145: 1219–1228. PMID: 9093870

35. Pritchard JK, Stephens M, Donnelly P. Inference of population structure using multilocus genotype data. Genetics. 2000; 155: 945–959. PMID: 10835412

36. Hubisz MJ, Falush D, Stephens M, Pritchard JK. Inferring weak population structure with the assistance of sample group information. Mol Ecol Resour. 2009; 9: 1322–1332. doi: 10.1111/j.1755-0998.2009.02591.x PMID: 21564903

37. Kopelman NM, Mayzel J, Jakobsson M, Rosenberg NA, Mayrose I. CLUMPAK: a program for identifying clustering modes and packaging population structure inferences across K. Mol Ecol Resour. 2015; 15: 1179–1191. Available: http://clumpak.tau.ac.il/ doi: 10.1111/1755-0998.12387 PMID: 25684545

38. Jakobsson M, Rosenberg NA. CLUMPP: A cluster matching and permutation program for dealing with label switching and multimodality in analysis of population structure. Bioinformatics. 2007; 23: 1801–1806. doi: 10.1093/bioinformatics/btm233 PMID: 17485429

39. Evanno G, Regnaut S, Goudet J. Detecting the number of clusters of individuals using the software STRUCTURE: A simulation study. Mol Ecol. 2005; 14: 2611–2620. doi: 10.1111/j.1365-294X.2005.02553.x PMID: 15969739

40. Earl DA, vonHoldt BM. STRUCTURE HARVESTER: A website and program for visualizing STRUCTURE output and implementing the Evanno method. Conserv Genet Resour. 2012; 4: 359–361. Available: http://taylor0.biology.ucla.edu/structureHarvester/ doi: 10.1007/s12686-011-9548-7

41. Bruno WJ, Socci ND, Halpern L. Weighted neighbor joining: a likelihood-based approach to distance-based phylogeny reconstruction. Mol Biol Evol. 2000; 17: 189–197. doi: 10.1093/oxfordjournals.molbev.a026231 PMID: 10666718

42. Cornuet JM, Santos F, Beaumont M, Robert CP, Marin JM, Balding DJ, et al. Inferring population history with DIY ABC: A user-friendly approach to approximate Bayesian computation. Bioinformatics. 2008; 24: 2713–2719. doi: 10.1093/bioinformatics/btn514 PMID: 18842597

43. Cornuet JM, Pudlo P, Veyssier J, Dehne-Garcia A, Gautier M, Leblois R, et al. DIYABC v2.0: A software to make approximate Bayesian computation inferences about population history using single nucleotide polymorphism, DNA sequence and microsatellite data. Bioinformatics. 2014; 30: 1187–1189. doi: 10.1093/bioinformatics/btt763 PMID: 24389659

44. Estoup A, Jarne P, Cornuet JM. Homoplasy and mutation model at microsatellite loci and their consequences for population genetics analysis. Mol Ecol. 2002; 11: 1591–1604. doi: 10.1046/j.1365-294x.2002.01576.x PMID: 12207711

45. Garza JC, Williamson EG. Detection of reduction in population size using data from microsatellite loci. Mol Ecol. 2002; 10: 305–318.

46. Excoffier L, Estoup A, Cornuet JM. Bayesian analysis of an admixture model with mutations and arbitrarily linked markers. Genetics. 2005; 169: 1727–1738. doi: 10.1534/genetics.104.036236 PMID: 15654099

47. Chung MY, López-Pujol J, Chung JM, Kim K-J, Chung MG. Low within population genetic variation and high among population differentiation in *Cyrtomium falcatum* (Lf) C. Presl (Dryopteridaceae) in southern Korea: Inference of population-establishment history. Am Fern J. 2012; 102: 256–272. doi: 10.1640/0002-8444-102.4.256

48. Tsuda Y, Nakao K, Ide Y, Tsumura Y. The population demography of *Betula maximowicziana*, a cooltemperate tree species in Japan, in relation to the last glacial period: its admixture-like genetic structure is the result of simple population splitting not admixing. Mol Ecol. 2015; 24: 1403–1418. doi: 10.1111/mec.13123 PMID: 25706115

49. Semerikov VL, Semerikova SA, Polezhaeva MA, Kosintsev PA, Lascoux M. Southern montane populations did not contribute to the recolonization of West Siberian Plain by Siberian larch (*Larix sibirica*): a range-wide analysis of cytoplasmic markers. Mol Ecol. 2013; 22: 4958–4971. doi: 10.1111/mec.12433 PMID: 24033458

50. Sakaguchi S, Bowman DMJS, Prior LD, Crisp MD, Linde CC, Tsumura Y, et al. Climate, not Aboriginal landscape burning, controlled the historical demography and distribution of fire-sensitive conifer populations across Australia. Proc Biol Sci. 2013; 280: 20132182. doi: 10.1098/rspb.2013.2182 PMID: 24174110

51. Hamrick JL, Godt MJW, Brown AHD, Clegg MT, Kahler AL, Weir BS, et al. Allozyme diversity in plant species. In Brown AHD, Clegg MT, Kahler AL, Weir BS, editors. Plant population genetics, breeding, and genetic resources. Sunderland: Sinauer Associates; 1990. pp. 43–63.

52. Pollak E. On the theory of partially inbreeding finite populations. I. Partial selfing. Genetics. 1987; 117: 353–360. PMID: 3666446

53. Nordborg M. Linkage disequilibrium, gene trees and selfing: an ancestral recombination graph with partial self-fertilization. Genetics. 2000; 154: 923–929. PMID: 10655241

54. Watano Y. Genetic life history of the homosporous fern *Osmunda lancea*. In Iwatsuki K, Raven PH, Bock WJ, editors. Modern aspects of species. Tokyo: Univ Tokyo Press; 1986. pp. 211–219.

55. Wubs EJ, de Groot GA, During HJ, Vogel JC, Grundmann M, Bermer P, et al. Mixed mating system in the fern *Asplenium scolopendrium*: implications for colonization potential. Ann Bot. 2010; 106: 583–590. doi: 10.1093/aob/mcq157 PMID: 20682575

56. De Groot GA, During HJ, Ansell SW, Schneider H, Bremer P, Wubs ERJ, et al. Diverse spore rains and limited local exchange shape fern genetic diversity in a recently created habitat colonized by long-distance dispersal. Ann Bot. 2012; 109: 965–978. doi: 10.1093/aob/mcs013 PMID: 22323427

57. Yuzawa Y. Assessment of damages on coastal and seashore plants in Fukushima Prefecture caused by Japan Tsunami following the Great East Japan Earthquake on 2011. J Phytogeogr Taxon. 2012; 61: 1–14.

58. Ranker T, Gemmill CE, Trapp PG. Microevolutionary patterns and processes of the native Hawaiian colonizing fern *Odontosoria chinensis* (Lindsaeaceae). Evolution. 2000; 54: 828–839. doi: 10.1111/j.0014-3820.2000.tb00083.x PMID: 10937256

59. Jiménez A, Holderegger R, Csencsics D, Quintanilla LG. Microsatellites reveal substantial among-population genetic differentiation and strong inbreeding in the relict fern *Dryopteris aemula*. Ann Bot. 2010; 106: 149–155. doi: 10.1093/aob/mcq094 PMID: 20495199

60. Chung MY, Moon MO, López-Pujol J, Maki M, Yamashiro T, Yukawa T, et al. Was Jeju Island a glacial refugium for East Asian warm-temperate plants? insights from the homosporous fern *Selliguea hastata* (Polypodiaceae). Am J Bot. 2013; 100: 2240–2249. doi: 10.3732/ajb.1300134 PMID: 24190948

61. Iwaizumi MG, Tsuda Y, Ohtani M, Tsumura Y, Takahashi M. Recent distribution changes affect geographic clines in genetic diversity and structure of *Pinus densiflora* natural populations in Japan. For Ecol Manage. 2013; 304: 407–416. doi: 10.1016/j.foreco.2013.05.026

62. Tsuda Y, Ide Y. Wide-range analysis of genetic structure of *Betula maximowicziana*, a long-lived pioneer tree species and noble hardwood in the cool temperate zone of Japan. Mol Ecol. 2005; 14: 3929–3941. doi: 10.1111/j.1365-294X.2005.02715.x PMID: 16262849

63. Tsuda Y, Sawada H, Ohsawa T, Nakao K, Nishikawa H, Ide Y. Landscape genetic structure of *Betula maximowicziana* in the Chichibu mountain range, central Japan. Tree Genet Genomes. 2010; 6: 377–387. doi: 10.1007/s11295-009-0256-3

64. Bystriakova N, Ansell SW, Russell SJ, Grundmann M, Vogel JC, Schneider H. Present, past and future of the European rock fern *Asplenium fontanum*: combining distribution modelling and population genetics to study the effect of climate change on geographic range and genetic diversity. Ann Bot. 2014; 113: 453–465. doi: 10.1093/aob/mct274 PMID: 24284816